

1       **Molecular Studies of Phages-*Klebsiella pneumoniae* in a Mucoid Environment:**  
2       **Innovative use of mucolytic agents prior to the administration of lytic phages**

3       Olga Pacios<sup>1,2</sup>, Lucía Blasco<sup>1,2</sup>, Concha Ortiz-Cartagena<sup>1,2</sup>, Inés Bleriot<sup>1,2</sup>, Laura Fernández-García<sup>1,2</sup>,  
4       María López<sup>1,2</sup>, Antonio Barrio-Pujante<sup>1,2</sup>, Álvaro Pascual<sup>2,3,6</sup>, Felipe Fernández Cuenca<sup>2,3,6</sup>, Luis  
5       Martínez-Martínez<sup>2,4,6</sup>, Belén Aracil<sup>5,6</sup>, Jesús Oteo-Iglesias<sup>2,5,6</sup> and María Tomás<sup>1,2\*</sup>

6

7       (1) Grupo de Microbiología Traslacional y Multidisciplinar (MicroTM)-Servicio de Microbiología Instituto  
8       de Investigación Biomédica A Coruña (INIBIC); Hospital A Coruña (CHUAC); Universidad de A Coruña  
9       (UDC), A Coruña;

10       (2) Grupo de Estudio de los Mecanismos de Resistencia Antimicrobiana (GEMARA) formando parte de la  
11       Sociedad Española de Enfermedades Infecciosas y Microbiología Clínica (SEIMC), Madrid;

12       (3) Unidad Clínica de Enfermedades Infecciosas y Microbiología Clínica, Hospital Universitario Virgen  
13       Macarena, Instituto de Biomedicina de Sevilla (Hospital Universitario Virgen Macarena/CSIC/  
14       Universidad de Sevilla), Sevilla;

15       (4) Unidad de Microbiología Clínica, Hospital Universitario Reina Sofía, Departamento e Química Agrícola,  
16       Edafología y Microbiología, Universidad de Córdoba, Instituto de Investigación en Biomedicina  
17       Maimonides (IMIBIC), Córdoba;

18       (5) Laboratorio de Referencia e Investigación de Resistencias a Antibióticos e Infecciones Sanitarias, Centro  
19       Nacional de Microbiología, Instituto de Salud Carlos III, Majadahonda, Madrid;

20       (6) CIBER de Enfermedades Infecciosas (CIBERINFEC), Instituto de Salud Carlos III, Madrid;

21

22       \*Correspondence: María Tomás

23       Email: [MA.del.Mar.Tomas.Carmona@sergas.es](mailto:MA.del.Mar.Tomas.Carmona@sergas.es);

24       Tel.: +34 981176399; Fax: +34 981178273.

25

26

27

28

29

30

31

32       **Running title:** Phage-Host interactions in a mucoid environment

33       **Keywords:** **Keywords:** *K. pneumoniae*, lytic bacteriophages, phage resistance, co-evolution,  
34       mucin, N-acetyl cysteine.

35 **Abstract**

36 Mucins are important glycoproteins that form a protective layer throughout the gastrointestinal  
37 and respiratory tracts. There is scientific evidence of increase in phage-resistance in the presence  
38 of mucin for some bacterial pathogens. Manipulation in mucin composition may ultimately  
39 influence the effectiveness of phage therapy. In this work, two clinical strains of *K. pneumoniae*  
40 (K3574 and K3325), were exposed to the lytic bacteriophage vB\_KpnS-VAC35 in the presence and  
41 absence of mucin on a long-term co-evolution assay, in an attempt to mimic *in vitro* the exposure  
42 to mucins that bacteria and their phages face *in vivo*. Enumerations of the bacterial and phage  
43 counts at regular time intervals were conducted, and extraction of the genomic DNA of co-  
44 evolved bacteria to the phage, the mucin and both was performed. We determined the frequency  
45 of phage-resistant mutants in the presence and absence of mucin and including a mucolytic agent  
46 (N-acetyl L-cysteine, NAC), and sequenced these conditions using Nanopore. We phenotypically  
47 demonstrated that the presence of mucin induces the emergence of bacterial resistance against  
48 lytic phages, effectively decreased in the presence of NAC. In addition, the genomic analysis  
49 revealed some of the genes relevant to the development of phage resistance in long-term co-  
50 evolution, with a special focus on the mucoid environment. Genes involved in the metabolism of  
51 carbohydrates were mutated in the presence of mucin. In conclusion, the use of mucolytic agents  
52 prior to the administration of lytic phages could be an interesting therapeutic option when  
53 addressing *K. pneumoniae* infections in environments where mucin is overproduced.

54

55

56

57

58

59

60

61

62

63 **Introduction**

64 *Klebsiella pneumoniae* is a Gram-negative opportunistic pathogen that causes urinary tract,  
65 wound and soft tissue infections, pneumonia, and even life-threatening sepsis (1, 2). Moreover,  
66 the recent increase of carbapenemase-producing strains of *K. pneumoniae* worldwide, together  
67 with its ability to grow in biofilm and to acquire plasmids conferring antibiotic (multi)resistance,  
68 underlie the importance of developing innovative and effective strategies against *K. pneumoniae*  
69 infections (3, 4).

70 In this context, the use of bacteriophages (or phages), viruses that specifically target bacteria in a  
71 highly effective and safe manner, is being evaluated as a therapeutic approach against bacterial  
72 infections, especially antibiotic-resistant ones (4, 5). Nevertheless, just as it happens with  
73 antibiotics, the emergence of phage-resistant mutants is a major hurdle to the establishment of  
74 phage therapy (4, 6). Indeed, to counter phage infection, bacteria display several defence  
75 mechanisms: mutation of the receptor recognized by a particular phage to inhibit adsorption  
76 (surface mutation) (7), induction of programmed death cell, known as abortive infection (Abi) (8),  
77 translation of nucleases that specifically degrade the phage DNA (CRISPR-Cas, restriction-  
78 modification... (9, 10)), etc. Despite the inconvenience of resistant bacteria against phages, their  
79 compassionate use in clinics has been approved in many countries and has already saved many  
80 life-threatening infectious patients (11-13).

81 Cystic Fibrosis (CF), an autosomal recessive genetic disorder that produces mutations in the cystic  
82 fibrosis transmembrane conductance regulator (CFTR) protein, is characterized by an  
83 overproduction of viscous mucins, since lack of CFTR function reduces airway mucus fluidity and  
84 influences hydration and mucin viscosity in the airways (14). This allows the trapping of inhaled  
85 bacteria in the lungs and explains why CF patients often become colonized by pathogens from an  
86 early age, which can lead to chronic infections (15). Even if a few typical bacteria are traditionally  
87 involved in CF lung infections, such as *Staphylococcus aureus* and *Pseudomonas aeruginosa*, CF  
88 patients are susceptible to infection by other opportunistic pathogens, including *K. pneumoniae*  
89 (16, 17).

90 To improve therapeutic outcomes in phage therapy, the arising of phage-resistant bacteria in the  
91 complex *in vivo* context needs to be exploited. Furthermore, not many studies address the  
92 efficiency of phage in long-term evolutionary experiments, nor look at phage co-evolution during  
93 phage treatments, as reviewed by Moulton-Brown in 2018 (18).

94 One of the main components of the gastrointestinal and respiratory tracts are mucins. Mucins are  
95 high-molecular-weight proteins that are glycosylated and can be transmembrane (forming a  
96 protective “brush” border on the epithelium) or gel-forming (providing hydration and protection  
97 from shear stress) (19, 20). They protect the intestinal mucosa from physical contact with

98 commensal bacteria, as well as from invasion of intruders and pathogens (21) . Changes in mucin  
99 expression are relevant in inflammatory and neoplastic disorders of the gastrointestinal tract,  
100 being important in the etiology of some infectious diseases, such as *Helicobacter pylori* gastritis  
101 (22).

102 In the present work, we have used two bacteriemic-causing clinical isolates of *K. pneumoniae*,  
103 named K3574 and K3325, and exposed them to the lytic bacteriophage vB\_KpnS-VAC35 in the  
104 presence and absence of mucin on a long-term co-evolution assay, intending to study the phage  
105 resistance in a mucoid environment. We determined the relationship between mucin and the  
106 difficulties in applying phage therapy, and we included a mucolytic agent to improve the use of  
107 phages by avoiding the emergence of resistance.

108 **Results**

109 **Infectivity of phage vB\_KpnS-VAC35**

110 The two strains exhibiting the highest efficiency of plating (EOP) values (K3574 and K3325) were  
111 chosen for further assays (Figure 1a). Optical density growth curves showed good lytic activity of  
112 vB\_KpnS-VAC35 in these strains at a multiplicity of infection (MOI) of 0.1 (purple line) and 1  
113 (orange line) (Figure 1 b) and c, respectively). The isolate K3325 was less well infected by  
114 vB\_KpnS-VAC35 than the isolation host, K3574.

115 **Co-evolution of K3574 and K3325 with the phage vB\_KpnS-VAC35 in a mucoid environment**

116 For the co-evolution experiment, the initial bacterial inoculum was  $2 \times 10^8$  colonies forming units  
117 per mL (CFU/mL) for K3574 and  $10^8$  CFU/mL for K3325 (Figure 2). As we infected both cultures in  
118 the exponential growth phase at a MOI=1, the initial phage concentration was  $2 \times 10^8$  plaque  
119 forming units per mL (PFU/mL) and  $10^8$  PFU/mL, respectively (Figure 2). The CFU counts remained  
120 stable at around  $10^{10}$  CFU/mL for both strains at every condition tested, whereas the PFUs  
121 fluctuated slightly more: in what concerns the isolate K3574 co-adapted to the phage, PFU counts  
122 ranged from  $10^9$  PFU/mL at 1 day post-infection (dpi) to  $10^7$  PFU/mL at 15 dpi, whereas in the  
123 presence of mucin these counts reached  $10^8$  PFU/mL at 9 dpi, then slightly decreased till  $10^7$   
124 PFU/mL at 15 dpi (Figure 2a), which corresponds to the 1:100 dilution performed every day along  
125 the experiment. Regarding the isolate K3325, co-evolution lasted 6 days as the PFU numbers  
126 dropped to 0 in the absence of mucin (Figure 2b). Nonetheless, in the presence of this compound,  
127  $10^3$  PFU/mL of vB\_KpnS-VAC35 were assessed at 6 dpi.

128

129 **Assessment of phage-resistance:**

130 **a. Spot test**

131 With the aim to assess the effect that the presence of mucin in the media will have on the  
132 bacterial susceptibility to the adapted phages, a spot test of *K. pneumoniae* K3574 and K3325  
133 prior to the co-evolution (named as “WT” in Figure 3), but also co-evolved in the presence of  
134 mucin, the phage, and both during 15 and 6 days, respectively, was conducted. As expected, WT  
135 and mucin-adapted cells (K3574\_ad15\_m and K3325\_ad6\_m) were the only conditions in which  
136 phage-susceptibility was kept (Figure 3). However, we observed differences when comparing the  
137 infection established by the non-adapted phage (vB\_KpnS-VAC35\_WT) and the adapted ones  
138 (vB\_KpnS-VAC35\_ad15 and vB\_KpnS-VAC35\_ad15\_m), which were isolated after 15 days of co-  
139 evolution with K3574 and produced more turbid spots (Figure 3, middle and right columns). The  
140 presence of more colonies growing inside the lytic halos of vB\_KpnS-VAC35\_ad15\_m compared to  
141 the infection established by vB\_KpnS-VAC35\_ad15 suggested that mucin either impaired the  
142 ability of the phage to lyse, or it enhanced the bacterial defence to the phage (as it has already  
143 been documented in the literature for different microorganisms (23, 24)).

144 **b. Frequency of arising of resistant mutants in the presence of the mucolytic N-acetyl L-  
145 cysteine (NAC)**

146 To quantitatively assess the effect that the presence of mucin had during bacteria and phage co-  
147 evolution, we determined the frequency of phage-resistant mutants to vB\_KpnS-VAC35. A  
148 condition in which *K. pneumoniae* clinical isolates K3574 and K3325 were incubated in presence of  
149 NAC for 15 and 6 days, respectively, was included. Consistently with the infection curves of  
150 vB\_KpnS-VAC35 in these two strains, we obtained a higher frequency for K3325 than K3574  
151 (Figure 4, orange bar). In the case of phage-exposed bacteria, either in the presence of mucin,  
152 NAC, or only the phage, no statistical difference was observed (Figure 4). Importantly, cells  
153 exposed to NAC displayed a statistically significant reduction in this frequency compared to the  
154 cells exposed to mucin.

155 **Genomic analysis of *K. pneumoniae* strains before and after the co-evolution in the presence of  
156 mucin**

157 Genomic analysis of the clinical strain K3574 adapted to mucin, to the phage alone or to both  
158 agents, were performed.

159 The reference genome of this strain (BioSample code SAMEA3649560, European BioProject  
160 PRJEB10018) possesses 5,635,279 pb (5561 coding sequences) with a GC content of 57.1%, a  
161 sequence-type ST3647 and a capsular type KL30. We extracted the bacterial DNA at 15 dpi of this  
162 isolate co-evolved to the phage (K3574\_ad15\_P), to mucin (K3574\_ad15\_M) and to both  
163 (K3574\_ad15\_P+M).

164 A Venn diagram was used to visualize the different and overlapping protein clusters displayed by  
165 the four complete genomes taken into consideration (Figure 5 b). In total, 5000 common protein

166 clusters were found between the strain prior to co-evolution and bacteria co-evolved to the  
167 phage (K3574\_ad15\_P), whereas 4938 were found between K3574\_WT and the mucin-adapted  
168 cells (K3574\_ad15\_M), and 4947 common protein clusters between K3574\_WT and cells co-  
169 evolved to the phage in the presence of mucin (K3574\_ad15\_P+M). No specific protein clusters  
170 were found for the strain adapted only to mucin (K3574\_ad15\_M) and to phage and mucin  
171 together (K3574\_ad15\_P+M), while 3 unique protein clusters were found in the isolate co-evolved  
172 to the phage alone (K3574\_ad15\_P) (Figure 5 b).

173 Comparison of the genomes revealed important mutations (Figure 6, Table 1). Among the genes  
174 in which nucleotide changes were found, we highlight several interesting ones grouped into  
175 different categories: concerning the bacterial defense mechanisms to phage infection, a tRNA-  
176 guanosine (18)-2'-O-methyltransferase carrying a nucleotide deletion in the position 362 was  
177 found in the case of K3574\_ad15\_P and K3574\_ad15\_P+M, whereas the non-infected isolate  
178 (K3574\_ad15\_M) had the intact locus compared to the K3574\_WT. This change (c.-362G) leads to  
179 a frameshift mutation translated into two truncated versions of the methyltransferase.  
180 Furthermore, the antitoxin HigA displayed mutations in the phage-infected cultures  
181 (K3574\_ad15\_P and K3574\_ad15\_P+M) that led to two different truncated proteins, whereas the  
182 non-infected strain had fewer changes that led to a shorter, unique version. Furthermore, the  
183 autoinducer 2-binding protein LsrB presented the same nucleotide deletion in the strains that co-  
184 evolved to the phage, also corresponding to a frameshift mutation (therefore a truncated protein  
185 lacking 11 amino acids); this was absent in the isolate exposed only to mucin.

186 Mutations in the core gene involved in Type VI secretion system, *vgrG*, were found in these same  
187 two strains but absent in the strain adapted only to mucin (K3674\_ad15\_M). Similarly, the same  
188 changes were found in the coding sequence of the outer membrane protein Ail (*attachment*  
189 *invasion locus*) of K3574\_ad15\_P and K3574\_ad15\_P+M, being intact in the isolate  
190 K3574\_ad15\_M. Interestingly, *fhuA*, the gene encoding a ferrichrome transporter protein, showed  
191 a frameshift mutation that led to two truncated versions of this protein in K3574\_ad15\_P+M,  
192 whereas this mutation was absent in K3574\_ad15\_P and K3574\_ad15\_M.

193 Mutations were found in genes involved in the metabolism of carbohydrates only for the strains  
194 adapted 15 days to mucin alone and to the phage in presence of mucin. For instance, nucleotide  
195 changes were observed in the gene *licC*, involved in the phosphoenolpyruvate-dependent sugar  
196 phosphotransferase system (PTS), in *rbsA*, *rbsB* and *fruK*, encoding the ribose and fructose import  
197 ATP-binding proteins RbsA/RbsB and FruK, respectively, or in *mall*, encoding a maltose regulon  
198 regulatory protein. More nucleotide changes in other relevant genes are reported in Table 1.

199 **Discussion**

200 Most of the works studying the interactions between pathogenic bacteria and their phages are  
201 generally carried out in well-defined laboratory conditions. However, these microbes in a natural  
202 environment develop complex interactions on mucosal surfaces of the vertebrate host (23). In  
203 2022, de Freitas *et al.* demonstrated that co-evolution of *Flavobacterium columnare* to its virulent  
204 phage V156 in presence of mucin dramatically increased the acquisition of spacers in the CRISPR  
205 arrays of *F. columnare* (23), thus increasing immunity to this phage. This work highlights the need  
206 to consider both biotic and abiotic variables if bacteriophages are to be used therapeutically. It is  
207 thus essential to take a close look at the study of how mucins and other mucosal components  
208 influence the acquisition of bacterial resistance towards lytic phages, so that the therapeutic  
209 potential of these could be better understood in the *in vivo* system.

210 Along the co-evolution performed with *K. pneumoniae* isolates K3574 and K3325, we observed  
211 that phage mutants arose at the first day post-infection (Figure 2), similar to what has been  
212 claimed in previous co-evolution works (25). Interestingly, both phage production (from 1 dpi  
213 onwards) and evolved *K. pneumoniae* populations seemed to stabilize over the days, consistently  
214 with other studies (26). This is likely due to the fact that vB\_KpnS-VAC35 selects for resistant  
215 bacterial mutants. Due to its gelatinous nature, mucin limits the diffusion of bacteria through this  
216 space and facilitates the interaction of phages with bacteria, a less well-studied function but  
217 already documented in literature (23, 27). In 2013, Barr *et al.* proposed a model in which  
218 bacteriophages would bind to mucins using the Ig-like domains present in many structural  
219 proteins, concentrate there, and protect humans and other metazoans against bacterial invaders  
220 (27, 28). Taken together, these two reasons could explain why the phage counts were higher in  
221 the presence of mucin than in the absence of this compound (Figure 2).

222 Interestingly, when the lytic phage was co-evolved to K3574 in the mucoid environment  
223 (vB\_KpnS-VAC35\_ad15\_m), it showed an impaired infection ability compared to the adapted  
224 phage in the absence of mucin (vB\_KpnS-VAC35\_ad15) (Figure 3). As expected, no spot was visible  
225 for the cells exposed to the phage either in the presence or the absence of mucin, leading to the  
226 conclusion that resistance arose as a result of the co-evolution process. We phenotypically  
227 confirmed that mucin increased the frequency of resistant mutants for *K. pneumoniae* K3574 and  
228 K3325 strains. Furthermore, NAC effectively reduced this frequency in the case of the cells  
229 incubated with this mucolytic (Figure 4). This resistant phenotype could be due to modification of  
230 the phage receptor; however, as this strategy represents an important fitness cost for bacteria,  
231 these have developed other strategies to avoid phage attachment (29). For instance, receptors  
232 can be masked, preventing recognition while retaining function. Capsules or exopolysaccharides  
233 provide phage resistance in *Staphylococcus* spp. (30), *Pseudomonas* spp. and *K. pneumoniae* (31),

234 and these bacterial structures can be favored in the presence of mucosal components such as  
235 mucins.

236 The analysis of protein clusters suggested that the presence of the phage in this long-term co-  
237 evolution experiment was the main driver in the acquisition of mutations. The genomic analysis of  
238 *K. pneumoniae* K3574 adapted to the phage alone and in presence of mucin revealed mutations in  
239 some proteins involved in the bacterial defense to phages, such as methyltransferases, the HigA  
240 antitoxin, the *quorum sensing* autoinducer LsrB or the type 6 secretion system VgrG, as reported  
241 in other works (32, 33) (Figure 6). In the presence of mucin, mutations were observed in the genes  
242 encoding proteins that were involved in the carbohydrates metabolism, such as in the PTS system,  
243 which is a major carbohydrate active-transport system that catalyzes the phosphorylation of  
244 incoming sugar substrates concomitant with their translocation across the cell membrane (34).

245 Since changes concerning the synthesis, secretion or structure of mucins have been linked to  
246 gastrointestinal and respiratory disorders, manipulation of mucin may ultimately influence the  
247 microbiota and the effectiveness of phage therapy for bacterial imbalances (21), and the use of a  
248 mucolytic agent as an adjuvant of lytic phages could be an interesting therapeutic option to take  
249 into consideration. It has been shown that the presence of bacteria upregulates mucin production  
250 and enhances their encapsulation by mucin in the colon, so this could be even more important in  
251 CF patients in which overproduction of mucins leads to lung chronic infections (35). Importantly,  
252 the trade-off costs that phage pressure and co-evolution represent for bacteria might render  
253 them less virulent in case of mutations in surface virulence factors, so maximizing the fitness costs  
254 that come with co-evolution may ultimately enhance the long-term efficacy of phage therapy.  
255 Optimization of these fitness costs could be a relevant factor to enhance the patient's prognosis  
256 (36).

257 All in all, this study sheds some light in the phage resistance behavior that might be expected for  
258 some clinical strains of *K. pneumoniae* in a mucoid environment, and takes a deeper look at the  
259 increase resistance that mucins induce to phages, already reported in literature (23). Evolutionary  
260 dynamics between bacterial pathogens and their natural predators in *in vivo* environments where  
261 mucin overproduction occurs deserve further investigation, which could help clinicians to predict  
262 the success of a particular phage administered to counteract infections. Finally, our results  
263 showed an innovative to option could be the application of mucolytic agents prior to the  
264 administration of lytic phages against by *K. pneumoniae* infections environments where mucin is  
265 overproduced as in cystic fibrosis disease. However, would be necessary to carry out more studies  
266 that include broad number clinical isolates to confirm this innovative therapeutic option.

267 **Materials and methods**

268 **Bacterial strains and growth conditions**

269 *K. pneumoniae* clinical strains K3574 and K3325 came from the National Centre for Microbiology  
270 (Carlos III Health Institute, Spain) previously analyzed<sup>23</sup>. All the bacterial strains were cultivated  
271 using Luria-Bertani broth (LB, 1% tryptone, 0.5% yeast extract and 0.5% NaCl). When required,  
272 purified mucin from porcine stomach (SigmaAldrich®), previously diluted in distilled water and  
273 autoclave-sterilized, was added at a final concentration of 1 mg/mL. NAC was also purchased from  
274 SigmaAldrich®, diluted with nuclease-free water, filter-sterilized and added to a final concentration  
275 of 10 mM.

276 **Establishment of the infectivity of the phage**

277 **a. Efficiency of plating (EOP)**

278 The EOP assay was done as previously described by Kutter *et al.*<sup>24</sup>, calculated as the ratio between  
279 the phage titre (PFU/mL) in the test strain and the titre in the isolation host (*K. pneumoniae*  
280 K3574). For both assays, TA-soft medium (1% tryptone, 0.5% NaCl and 0.4% agar) was used to  
281 make plates by the top-agar method<sup>25</sup>. Strains exhibiting susceptibility to phage infection in the  
282 spot test performed by Bleriot *et al.* in a previous work<sup>23</sup> were selected for the EOP assay.

283 **b. Infection curves**

284 To assess the lytic capacity of vB\_KpnS-VAC35<sup>23</sup>, infection curves at different MOI were performed.  
285 Overnight cultures of the clinical isolates of *K. pneumoniae* K3574 and K3325 were diluted 1:100 in  
286 LB broth and then incubated at 37°C at 180 rpm until an early exponential phase (OD<sub>600 nm</sub> = 0.3-  
287 0.4) was reached. Then, vB\_KpnS-VAC35 was added to the cultures at MOI of 0.1 and 1, and OD<sub>600</sub>  
288 nm was measured during 6 hours at 1-hour intervals.

289 **Co-evolution between vB\_KpnS-VAC35 and *K. pneumoniae* strains K3574 and K3325**

290 The bacterial strains were incubated in 20 mL LB-containing flasks at 37°C and 180 rpm for 6  
291 (K3325) or 15 days (K3574); the flasks were infected with vB\_KpnS-VAC35 at a MOI=1 in the  
292 presence and absence of porcine mucin at a final concentration of 1 mg/mL, and a non-infected  
293 control of the bacterial isolate growing in presence of 1 mg/mL mucin was included. The infections  
294 with the phage were performed at OD≈ of 0.4. From this moment and every 24 hours, each  
295 condition was 1:100 diluted in fresh LB medium, containing 1 mg/mL mucin when required, and  
296 enumeration of CFU and PFU was performed. For the CFU enumeration, 1 mL aliquots of bacterial  
297 cultures were serially diluted in the saline buffer then plated on LB-agar plates (100 µL) and  
298 incubated overnight. For the PFU assessment, 1 mL aliquots were centrifuged 5 min at maximum  
299 speed (14000 rpm) for the collection of phage particles in the supernatant. Serial dilutions of  
300 these PFU were performed in SM buffer (100 mM NaCl, 10 mM MgSO<sub>4</sub>, 20 mM Tris-HCl, pH 7.5),  
301 then 10 µL of the pertinent dilutions were plated by the double-layer method (37). Two flasks per  
302 condition were considered as biological duplicates.

303 **Assessment of phage resistance**

304 **a. Spot test**

305 The spot test assay was undertaken as described by Raya *et al.* (38). We used vB\_KpnS-VAC35 WT,  
306 vB\_KpnS-VAC35\_ad15 and vB\_KpnS-VAC35\_ad15\_m phages, that is prior to co-evolution, and  
307 adapted to K3574 during 15 days in the absence and presence of mucin, respectively.

308 **b. Calculation of the frequency of phage-resistant mutants**

309 The frequency of resistant mutants was calculated as previously described by Lopes *et al.* (39).  
310 Overnight cultures of the strains K3574 and K3325 at the different conditions evaluated were  
311 diluted 1:100 in LB and grown to an OD<sub>600nm</sub> of 0.7. An aliquot of 1 mL of the culture containing 10<sup>8</sup>  
312 CFU/mL was serially diluted, and the corresponding dilutions were mixed with 100 µL of vB\_KpnS-  
313 VAC35 at 10<sup>9</sup> PFU/mL, then plated by the double-layer method in TA medium. The plates were  
314 incubated at 37°C for 24h, then the colonies of resistant mutants were enumerated. The mutation  
315 rate was calculated by dividing the number of resistant bacteria (growing in the presence of the  
316 phage) by the total number of bacteria plated in conventional LB-agar (100 µL).

317 **Genomic DNA extraction and whole-genome sequencing**

318 The DNeasy Blood & Tissue Kit (Qiagen®) was used for extracting the genomic DNA of bacterial  
319 cultures co-evolved 15 dpi with the vB\_KpnS-VAC35 alone (K3574\_ad15\_P), in the presence of  
320 mucin (K3574\_ad15\_P+M) and exposed 15 days to mucin (K3574\_ad15\_M), following the  
321 manufacturer's instructions. Samples were quantified with a Qubit 3.0 fluorometer using a Qubit  
322 dsDNA HS Assay Kit and with a Nanodrop spectrophotometer to evaluate the DNA purity. The  
323 MinION MK1C instrument with the Rapid Barcoding Kit (SQK-RBK004) were employed, following  
324 the manufacturer's protocol and using a MinION flow cell v.9.4.1.

325 **Bioinformatic analysis**

326 Basecalling was performed using GUPPY (Version 5.0.7 Super-accuracy model (SUP)) to generate  
327 fastQ sequencing reads from electrical data (the fast5 files generated by MinION). The reads were  
328 then further subsampled according to their barcodes and *de novo* assembled using Unicycler.  
329 Further analyses were performed after visualization of circular assembled genomes using  
330 Bandage. Draft assemblies were corrected by using iterative rounds of polishing with the Racon  
331 error correction software. Annotations were performed using Prokka (40), and insertions,  
332 deletions and other SNPs were called using the structural variant caller Snippy (v1.0.11). The  
333 presence and absence of intact genetic sequences were analyzed using Roary and Orthovenn2.  
334 OrthoVenn2 (<http://www.bioinfogenome.net/OrthoVenn/>) was used to compare the proteins of  
335 the four complete genomes using the files generated by Prokka analysis. Fasta files obtained after  
336 annotation were surveilled for indels using the blastn and blastp tools from the NCBI and  
337 compared to the reference genome (for K3574\_WT, BioSample code SAMEA3649560 included in

338 the European BioProject PRJEB10018). The workflow taken from Nanopore sequencing to the  
339 genomic analysis is summarized in Figure 5 a.

340

341

342 **Funding**

343 This study has been funded by Instituto de Salud Carlos III (ISCIII) through the projects PI19/00878  
344 and PI22/00323 and co-funded by the European Union, and by the Study Group on Mechanisms  
345 of Action and Resistance to Antimicrobials, GEMARA (SEIMC). (SEIMC, <http://www.seimc.org/>).  
346 This research was also supported by CIBERINFEC (CIBER21/13/00095) and by *Personalized and*  
347 *precision medicine* grant from the Instituto de Salud Carlos III (MePRAM Project, PMP22/00092).  
348 M. Tomás was financially supported by the Miguel Servet Research Programme (SERGAS and  
349 ISCIII). O. Pachos, L. Fernández-García and M. López were financially supported by the grants  
350 IN606A-2020/035, IN606B-2021/013 and IN606C-2022/002, respectively (GAIN, Xunta de Galicia).  
351 I.Bleriot was financially supported by the pFIS program (ISCIII, FI20/00302). Finally, to thank to  
352 PIRASOA laboratory which is the reference laboratory for molecular typing of nosocomial  
353 pathogens and detection of mechanisms of resistance to antimicrobials of health interest in  
354 Andalusia, Virgen Macarena Hospital, Seville, to send us the clinical isolates.

355 **Transparency declarations**

356 The authors declare not to have conflict of interest

357

358 **Figure legends**

359 **Figure 1:** a) EOP of vB\_KpnS-VAC35 on some clinical isolates of *K. pneumoniae*, with different  
360 capsular type. b) and c) Infection curves of clinical isolates K3574 and K3325 by the lytic phage  
361 vB\_KpnS-VAC35, prior to co-evolution, at MOI 0.1 and 1.

362 **Figure 2:** Titration of the colony forming units (CFU, left Y-axis) and plaque forming units (PFU,  
363 right Y-axis) per mL during the co-evolution experiments between clinical isolates K3574 (a)) and  
364 K3325 (b)) and the lytic bacteriophage vB\_KpnS-VAC35, in the absence and presence of mucin (1  
365 mg/mL).

366 **Figure 3:** Spot tests of phages prior to co-evolution (vB\_KpnS-VAC35 WT), co-evolved to K3574 in  
367 the absence and in the presence of mucin (vB\_KpnS-VAC35\_ad15 and vB\_KpnS-VAC35\_ad15\_m,  
368 respectively). A) Spot test using the clinical isolate *K. pneumoniae* K3574 WT, adapted 15 days to  
369 the phage, to mucin and to both. B) Spot test using the clinical isolate *K. pneumoniae* K3325 WT,  
370 adapted 6 days to the phage, to mucin and to both.

371 **Figure 4:** Frequency of occurrence of resistant mutants for *K. pneumoniae* K3574 (a) and *K.*  
372 *pneumoniae* K3325 (b). The statistical analysis (t-test) was performed with GraphPad Prism v.9.  
373 \*\*: p-value < 0.001; \*: p-value 0.042. Absence of asterisk corresponds to non-statistical  
374 significance.

375 **Figure 5:** a) Schematic representation of the workflow followed from the whole-genome  
376 sequencing with Nanopore till the analyse of the genomic sequences. B) Venn diagram performed  
377 with OrthoVenn2 to visualize the overlapped and unique protein clusters in the four complete  
378 genomes analysed.

379 **Figure 6:** Comparative genomic analysis of *K. pneumoniae* K3574 co-evolved to phage alone (pink  
380 ring), mucin alone (blue ring) and both (green ring) constructed with the BLAST Ring Image  
381 Generator (BRIG). The sequence corresponding to K3574\_WT is located on the innermost side  
382 (black ring). The double ring adjacent to the reference sequence represents the GC content (black)  
383 and the GC skew (dark purple and dark green). The white parts of the rings represent absent or  
384 divergent content and are squared in black.

385 **Table 1:** Mutations found in the four complete genomes analyzed, grouped into different  
386 categories by function. “c.” corresponds to the nucleotide changes found in the coding sequences,  
387 while “p.” stands for protein sequences. Asterisks indicate that mutations are the same between  
388 the studied conditions.



390  
391  
392  
393  
394  
395  
396  
397  
398  
399  
400  
401  
402  
403  
404  
405  
406  
407  
408

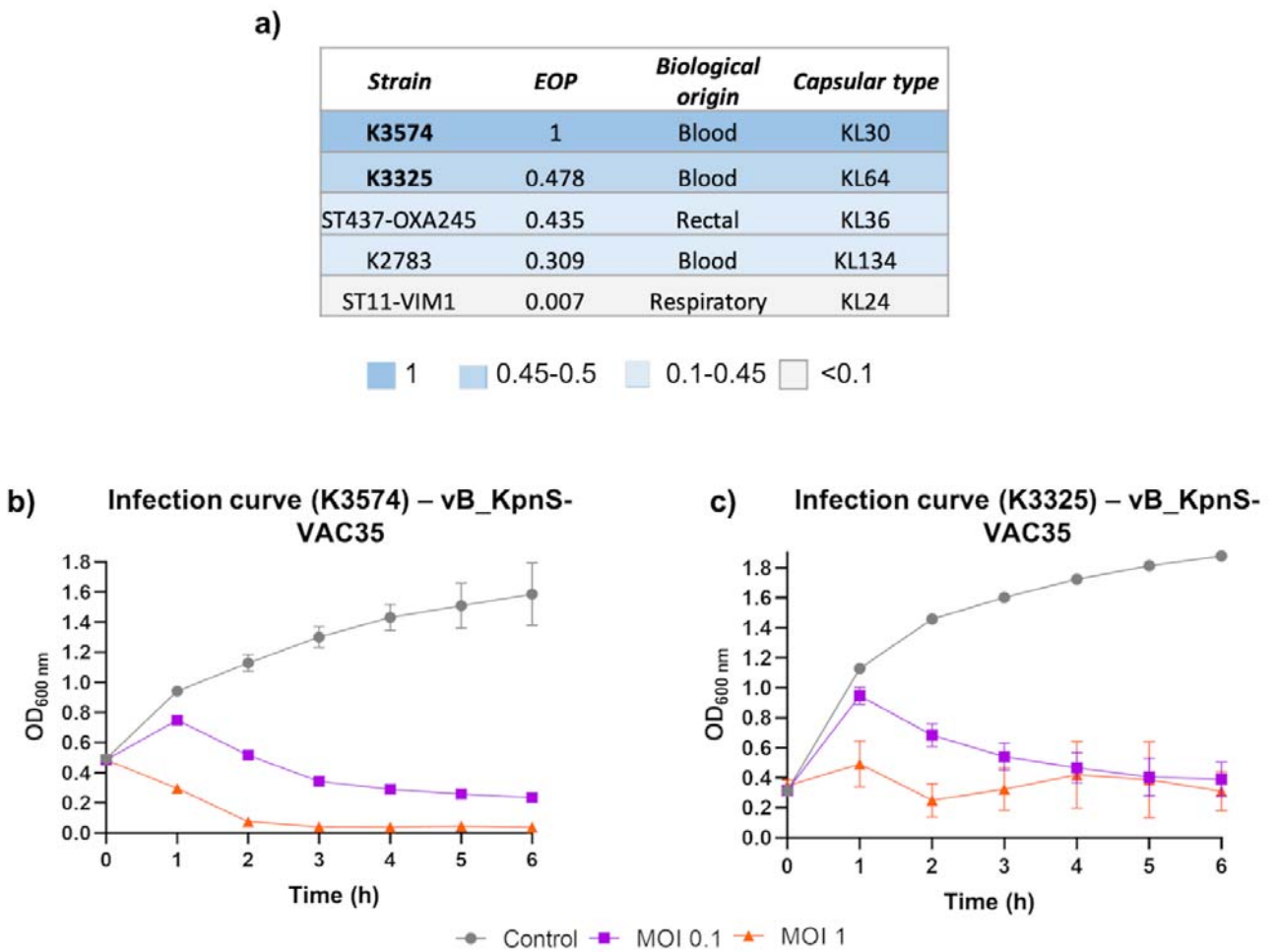
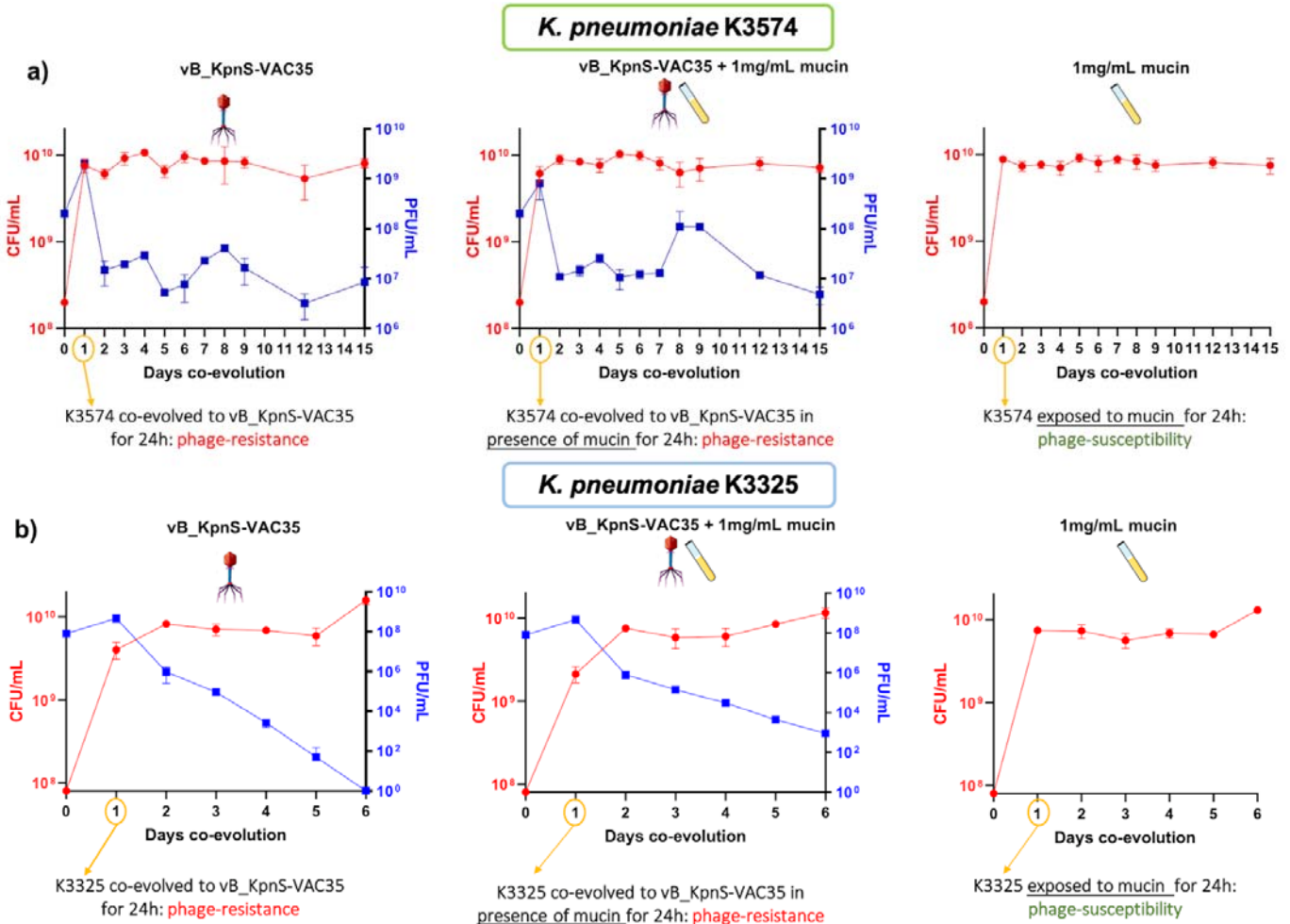
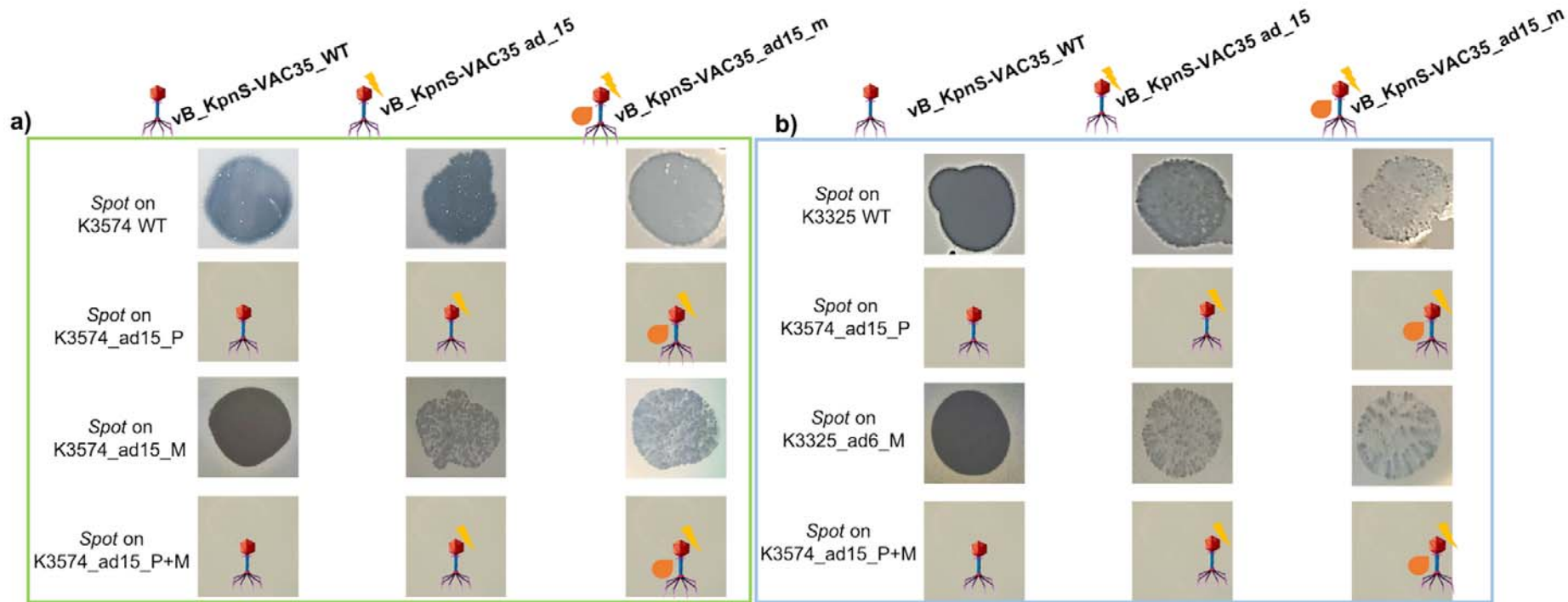


Figure 1

409



410 **Figure 2**



411

412 **Figure 3**

413

414

415

416

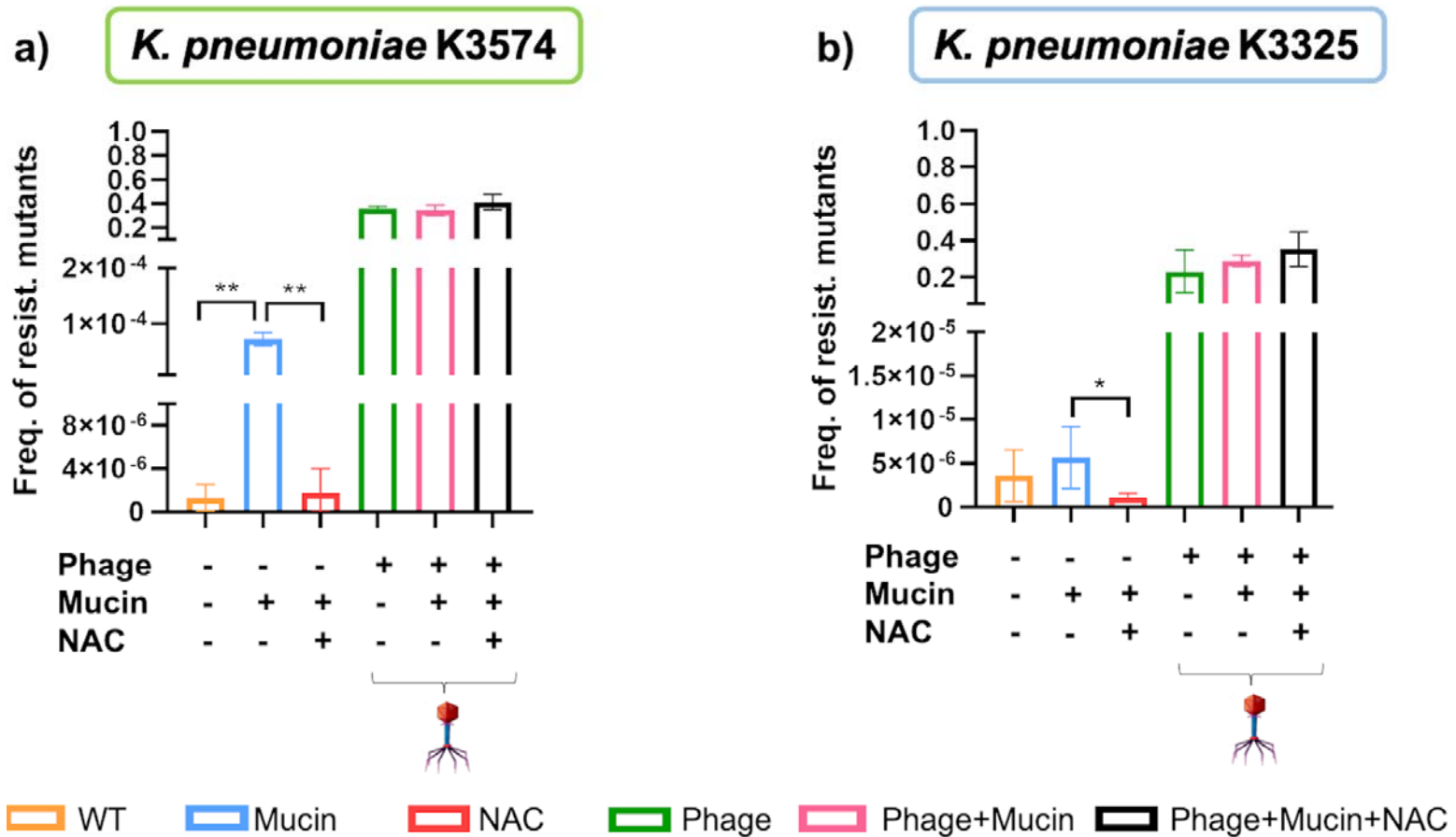
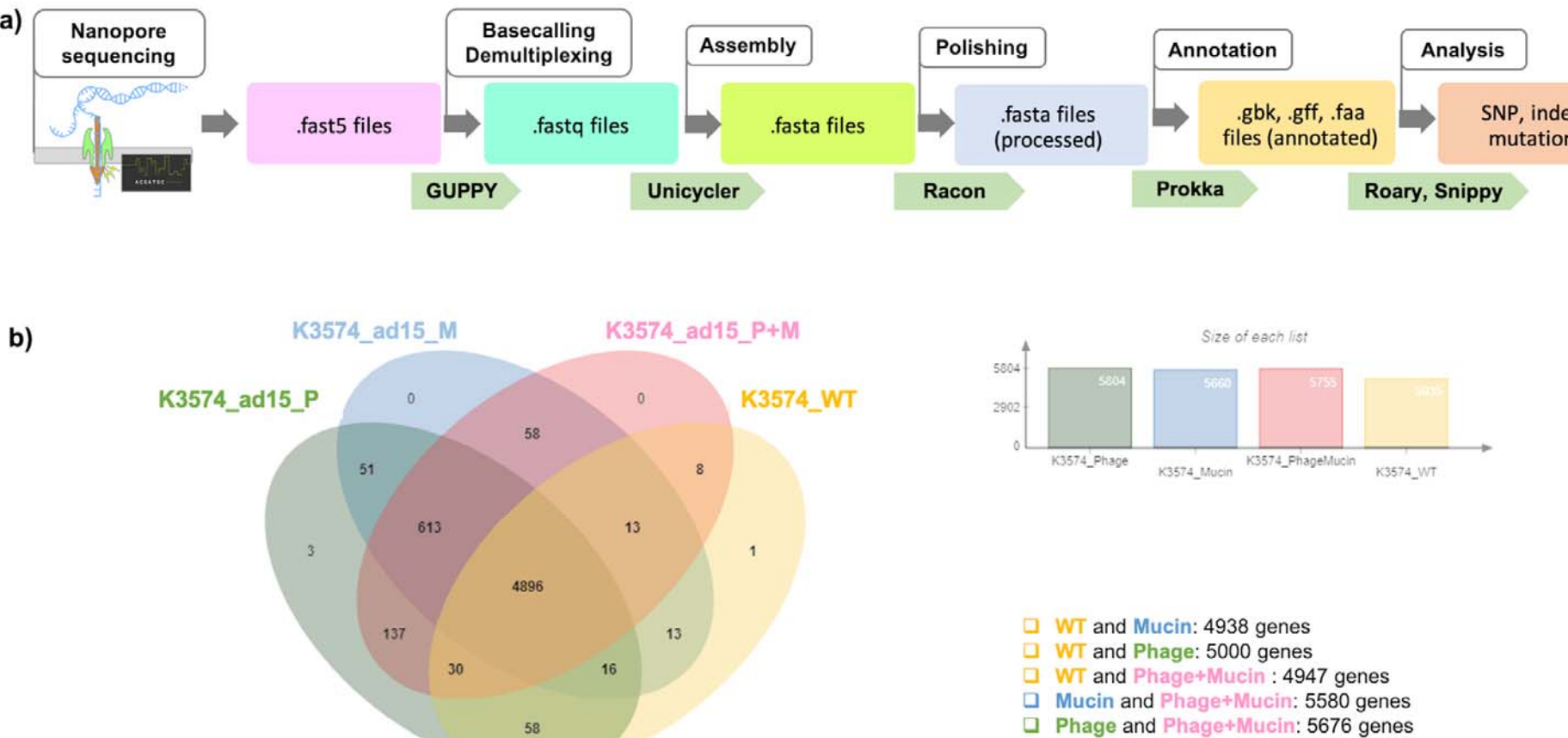


**Figure 4**

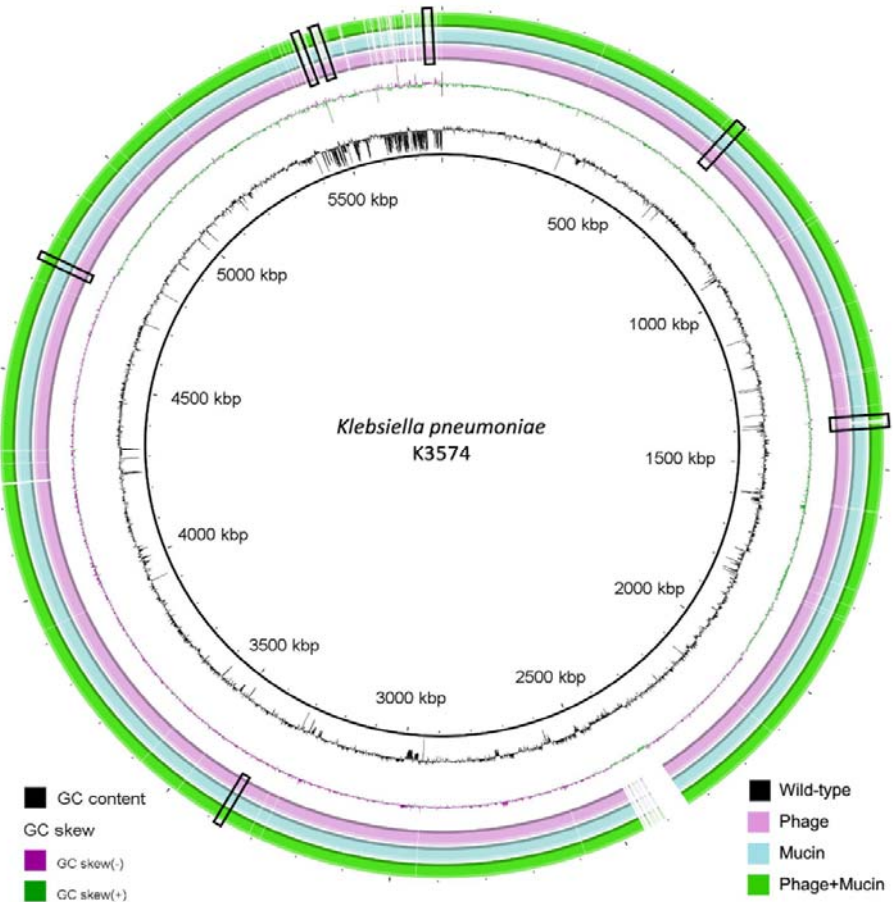


433

434

435 **Figure 5**

436



437

438 **Figure 6**

19

**Table 1:**

	K3574_ad15_P (co-evolved with the phage)	K3574_ad15_M (non-infected, exposed to mucin)	K3574_ad15_P+M (co-evolved with the phage in presence of mucin)
<b>Anti-phage bacterial defense</b>			
Anti-toxin HigA	c.T66-, c.T114-, c.A152- c.C199T, c.C201A. 2 truncated proteins	c.T66-, c.T105-, c.T106-. 1 protein FDNEPAPDTPEGDF>LIMNLLRRRKKG-I	c.T66-, c.T114-, c.A152- c.C199T, c.C201A. 2 truncated proteins
CRISPR-associated endonuclease/helicase Cas3	None	None	c.A2130-, c.A1236-, p.ALLAEVGVGTLQDQLL>RYSLKL-VSVLISF
tRNA (guanosine(18)-2'-O)-methyltransferase	c.A362-	None	c.A362-
<b>Quorum sensing</b>			
Autoinducer 2-binding protein LsrB	c.G341-, truncated protein (11 aa less)	None	c.G341-, truncated protein (11 aa less)
<b>PG synthesis</b>			
Murein DD-endopeptidase MepS/Murein LD-carboxypeptidase	Truncated version (lack 28 aas)	None	Truncated version (lack 28 aas)
FtsI Peptidoglycan D-transpeptidase	c.A1495- p.W501V	None	c.A1495- p.W501V
<b>LPS biosynthesis</b>			
undecaprenyl phosphate-alpha-4-amino-4-deoxy-L-arabinose arabinosyl transferase	None	None	c.G664-, 2 truncated proteins (263 and 251 aas)
lipopolysaccharide assembly protein LptD	Truncated version c.G1861- ; p.*	None	None
<b>Efflux</b>			
BepE (efflux)	Shorter protein	Deletions in positions 370,371,381,1641 (truncated protein, p.G125W, p.v126R, p.v127S)	Deletions in positions 370,371,381,1641 (truncated protein, p.G125W, p.v126R, p.v127S)
BepG (efflux)	Deletion c.2867 (truncated protein)	Truncated version c.C1937T, Truncated protein	Deletion c.2867 (truncated protein)

<b>Multidrug efflux transporter transcriptional repressor AcrR</b>	Mutations p.K53R, p.K55N, p.K80N, p.N54I, p.N60T	Shorter version	Mutations p.K53R, p.K55N, p.K80N, p.N54I, p.N60T
<b>Multidrug resistance protein MdtM</b>	LGVLRDFRNVFRNRF>WACCAIFATSFATASF	c.202 GILH>PRCRM	Lack 83 aa
<b>Secretion systems</b>			
<b>T2SS protein F</b>	Truncated version	Truncated version	Truncated version
<b>T6SS VgrG1</b>	c.G2182-, Truncated protein( p.N768*)	None	c.G2182-, Truncated protein( p.N768*)
<b>Fimbrial proteins</b>			
<b>Fimbrial chaperone YadV</b>	c.C624-; Truncated protein p.P210L	Truncated protein	Truncated protein
<b>putative hydrolase YxeP (active on CN bonds)</b>	Truncated version	None	Truncated version
<b>Outer membrane usher protein HtrE</b>	Deletion 2205 (truncated protein)	c.C2202-. Shorter sequence	Deletion 2205 (truncated protein)
<b>Xylose import ATP-binding protein XylG</b>	Truncated version	Truncated version	Truncated version
<b>Putative receptors</b>			
<b>Outer membrane channel OprM</b>	Insertion in position 177 (1 truncated protein, lacking 18 aa)	c.G539-	Insertion in position 177 (1 truncated protein, lacking 18 aa)
<b>Ail/Lom family outer membrane protein</b>	Truncated version (65 aa)	None	Truncated version (65 aa)
<b>Receptor vitamin B12 BtuB</b>	Truncated version; truncated protein	None	Truncated version deletion 1234, truncated protein p.S414P, p.L415S
<b>Ferrichrome FhuA</b>	None	None	2 truncated versions
<b>Ferrienterobactin receptor (FepA)</b>	3 truncated versions *	2 truncated versions	3 truncated versions *
<b>Virulence factors</b>			
<b>Ail/Lom family outer membrane protein</b>	Deletion c.193- (truncated protein)	None	Deletion c.193- (truncated protein)

440

441

442

443

444 **References**

445 1. Kamruzzaman M, Iredell JR. 2019. CRISPR-Cas System in Antibiotic Resistance Plasmids  
446 in *Klebsiella pneumoniae*. *Front Microbiol* 10:2934.

447 2. Mackow NA, Shen J, Adnan M, Khan AS, Fries BC, Diago-Navarro E. 2019. CRISPR-Cas  
448 influences the acquisition of antibiotic resistance in *Klebsiella pneumoniae*. *PLoS One*  
449 14:e0225131.

450 3. Pacios O, Fernández-García L, Bleriot I, Blasco L, González-Bardanca M, López M,  
451 Fernández-Cuenca F, Oteo J, Pascual Á, Martínez-Martínez L, Domingo-Calap P, Bou G,  
452 Tomás M, (SEIMC) SGoMoAaRtAGobotSSoIDaCM. 2021. Enhanced Antibacterial  
453 Activity of Repurposed Mitomycin C and Imipenem in Combination with the Lytic  
454 Phage vB\_KpnM-VAC13 against Clinical Isolates of *Klebsiella pneumoniae*. *Antimicrob  
455 Agents Chemother* 65:e0090021.

456 4. Majkowska-Skrobek G, Markwitz P, Sosnowska E, Lood C, Lavigne R, Drulis-Kawa Z.  
457 2021. The evolutionary trade-offs in phage-resistant *Klebsiella pneumoniae* entail  
458 cross-phage sensitization and loss of multidrug resistance. *Environ Microbiol*.

459 5. Pacios O, Blasco L, Bleriot I, Fernandez-Garcia L, Gonzalez Bardanca M, Ambroa A,  
460 Lopez M, Bou G, Tomas M. 2020. Strategies to Combat Multidrug-Resistant and  
461 Persistent Infectious Diseases. *Antibiotics (Basel)* 9.

462 6. Uyttebroek S, Chen B, Onsea J, Ruythooren F, Debaveye Y, Devolder D, Spriet I,  
463 Depypere M, Wagemans J, Lavigne R, Pirnay JP, Merabishvili M, De Munter P,  
464 Peetermans WE, Dupont L, Van Gerven L, Metsemakers WJ. 2022. Safety and efficacy  
465 of phage therapy in difficult-to-treat infections: a systematic review. *Lancet Infect Dis*  
466 22:e208-e220.

467 7. Denes T, den Bakker HC, Tokman JI, Guldmann C, Wiedmann M. 2015. Selection and  
468 Characterization of Phage-Resistant Mutant Strains of *Listeria monocytogenes* Reveal  
469 Host Genes Linked to Phage Adsorption. *Appl Environ Microbiol* 81:4295-305.

470 8. Lopatina A, Tal N, Sorek R. 2020. Abortive Infection: Bacterial Suicide as an Antiviral  
471 Immune Strategy. *Annu Rev Virol* 7:371-384.

472 9. Castillo JA, Secaira-Morocho H, Maldonado S, Sarmiento KN. 2020. Diversity and  
473 Evolutionary Dynamics of Antiphage Defense Systems in *Ralstonia  
474 solanacearum* Species Complex. *Front Microbiol* 11:961.

475 10. Ambroa A, Blasco L, Lopez M, Pacios O, Bleriot I, Fernandez-Garcia L, Gonzalez de  
476 Aledo M, Ortiz-Cartagena C, Millard A, Tomas M. 2021. Genomic Analysis of Molecular  
477 Bacterial Mechanisms of Resistance to Phage Infection. *Front Microbiol* 12:784949.

478 11. Schooley RT, Biswas B, Gill JJ, Hernandez-Morales A, Lancaster J, Lessor L, Barr JJ, Reed  
479 SL, Rohwer F, Benler S, Segall AM, Taplitz R, Smith DM, Kerr K, Kumaraswamy M, Nizet  
480 V, Lin L, McCauley MD, Strathdee SA, Benson CA, Pope RK, Leroux BM, Picel AC,  
481 Mateczun AJ, Cilwa KE, Regeimbal JM, Estrella LA, Wolfe DM, Henry MS, Quinones J,  
482 Salka S, Bishop-Lilly KA, Young R, Hamilton T. 2017. Development and Use of  
483 Personalized Bacteriophage-Based Therapeutic Cocktails To Treat a Patient with a  
484 Disseminated Resistant *Acinetobacter baumannii* Infection. *Antimicrob Agents  
485 Chemother* 61.

486 12. Law N, Logan C, Yung G, Furr CL, Lehman SM, Morales S, Rosas F, Gaidamaka A,  
487 Bilinsky I, Grint P, Schooley RT, Aslam S. 2019. Successful adjunctive use of  
488 bacteriophage therapy for treatment of multidrug-resistant *Pseudomonas aeruginosa*  
489 infection in a cystic fibrosis patient. *Infection* 47:665-668.

490 13. Dedrick RM, Guerrero-Bustamante CA, Garlena RA, Russell DA, Ford K, Harris K,  
491 Gilmour KC, Soothill J, Jacobs-Sera D, Schooley RT, Hatfull GF, Spencer H. 2019.  
492 Engineered bacteriophages for treatment of a patient with a disseminated drug-  
493 resistant *Mycobacterium abscessus*. *Nat Med* 25:730-733.

494 14. Riquelme SA, Ahn D, Prince A. 2018. *Pseudomonas aeruginosa* and *Klebsiella  
495 pneumoniae* Adaptation to Innate Immune Clearance Mechanisms in the Lung. *J Innate  
496 Immun* 10:442-454.

497 15. Pletzer D, Mansour SC, Wuerth K, Rahanjam N, Hancock RE. 2017. New Mouse Model  
498 for Chronic Infections by Gram-Negative Bacteria Enabling the Study of Anti-Infective  
499 Efficacy and Host-Microbe Interactions. *mBio* 8.

500 16. Leão RS, Pereira RH, Folescu TW, Albano RM, Santos EA, Junior LG, Marques EA. 2011.  
501 KPC-2 carbapenemase-producing *Klebsiella pneumoniae* isolates from patients with  
502 Cystic Fibrosis. *J Cyst Fibros* 10:140-2.

503 17. Delfino E, Giacobbe DR, Del Bono V, Coppo E, Marchese A, Manno G, Morelli P,  
504 Minicucci L, Viscoli C. 2015. First report of chronic pulmonary infection by KPC-3-  
505 producing and colistin-resistant *Klebsiella pneumoniae* sequence type 258 (ST258) in  
506 an adult patient with cystic fibrosis. *J Clin Microbiol* 53:1442-4.

507 18. Moulton-Brown CE, Friman VP. 2018. Rapid evolution of generalized resistance  
508 mechanisms can constrain the efficacy of phage-antibiotic treatments. *Evol Appl  
509* 11:1630-1641.

510 19. Hansson GC. 2019. Mucus and mucins in diseases of the intestinal and respiratory  
511 tracts. *J Intern Med* 285:479-490.

512 20. Paone P, Cani PD. 2020. Mucus barrier, mucins and gut microbiota: the expected slimy  
513 partners? *Gut* 69:2232-2243.

514 21. Carroll-Portillo A, Lin HC. 2021. Exploring Mucin as Adjunct to Phage Therapy.  
515 *Microorganisms* 9.

516 22. Jass JR, Walsh MD. 2001. Altered mucin expression in the gastrointestinal tract: a  
517 review. *J Cell Mol Med* 5:327-51.

518 23. de Freitas Almeida GM, Hoikkala V, Ravantti J, Rantanen N, Sundberg LR. 2022. Mucin  
519 induces CRISPR-Cas defense in an opportunistic pathogen. *Nat Commun* 13:3653.

520 24. Green SI, Gu Liu C, Yu X, Gibson S, Salmen W, Rajan A, Carter HE, Clark JR, Song X,  
521 Ramig RF, Trautner BW, Kaplan HB, Maresso AW. 2021. Targeting of Mammalian  
522 Glycans Enhances Phage Predation in the Gastrointestinal Tract. *mBio* 12.

523 25. Oechslin F. 2018. Resistance Development to Bacteriophages Occurring during  
524 Bacteriophage Therapy. *Viruses* 10.

525 26. Rendueles O, de Sousa JAM, Rocha EPC. 2023. Competition between lysogenic and  
526 sensitive bacteria is determined by the fitness costs of the different emerging phage-  
527 resistance strategies. *Elife* 12.

528 27. Barr JJ, Auro R, Furlan M, Whiteson KL, Erb ML, Pogliano J, Stotland A, Wolkowicz R,  
529 Cutting AS, Doran KS, Salamon P, Youle M, Rohwer F. 2013. Bacteriophage adhering to  
530 mucus provide a non-host-derived immunity. *Proc Natl Acad Sci U S A* 110:10771-6.

531 28. Almeida GMF, Laanto E, Ashrafi R, Sundberg LR. 2019. Bacteriophage Adherence to  
532 Mucus Mediates Preventive Protection against Pathogenic Bacteria. *mBio* 10.

533 29. Wright RCT, Friman VP, Smith MCM, Brockhurst MA. 2019. Resistance Evolution  
534 against Phage Combinations Depends on the Timing and Order of Exposure. *mBio* 10.

535 30. Ohshima Y, Schumacher-Perdreau F, Peters G, Pulverer G. 1988. The role of capsule as  
536 a barrier to bacteriophage adsorption in an encapsulated *Staphylococcus simulans*  
537 strain. *Med Microbiol Immunol* 177:229-33.

538 31. Hao G, Shu R, Ding L, Chen X, Miao Y, Wu J, Zhou H, Wang H. 2021. Bacteriophage  
539 SRD2021 Recognizing Capsular Polysaccharide Shows Therapeutic Potential in  
540 Serotype K47 *Klebsiella pneumoniae* Infections. *Antibiotics (Basel)* 10.

541 32. Blasco L, López-Hernández I, Rodríguez-Fernández M, Pérez-Florido J, Casimiro-  
542 Soriguer CS, Djebara S, Merabishvili M, Pirnay J-P, Rodríguez-Baño J, Tomás M, López  
543 Cortés LE. 2023. Case report: Analysis of phage therapy failure in a patient with a  
544 *Pseudomonas aeruginosa* prosthetic vascular graft infection. *Frontiers in Medicine* 10.

545 33. Liu M, Hernandez-Morales A, Clark J, Le T, Biswas B, Bishop-Lilly KA, Henry M,  
546 Quinones J, Voegtly LJ, Cer RZ, Hamilton T, Schooley RT, Salka S, Young R, Gill JJ. 2022.

547 Comparative genomics of *Acinetobacter baumannii* and therapeutic bacteriophages  
548 from a patient undergoing phage therapy. *Nat Commun* 13:3776.

549 34. Deutscher J, Francke C, Postma PW. 2006. How phosphotransferase system-related  
550 protein phosphorylation regulates carbohydrate metabolism in bacteria. *Microbiol Mol  
551 Biol Rev* 70:939-1031.

552 35. Bergstrom K, Shan X, Casero D, Batushansky A, Lagishetty V, Jacobs JP, Hoover C,  
553 Kondo Y, Shao B, Gao L, Zandberg W, Noyovitz B, McDaniel JM, Gibson DL, Pakpour S,  
554 Kazemian N, McGee S, Houchen CW, Rao CV, Griffin TM, Sonnenburg JL, McEver RP,  
555 Braun J, Xia L. 2020. Proximal colon-derived O-glycosylated mucus encapsulates and  
556 modulates the microbiota. *Science* 370:467-472.

557 36. Mangalea MR, Duerkop BA. 2020. Fitness Trade-Offs Resulting from Bacteriophage  
558 Resistance Potentiate Synergistic Antibacterial Strategies. *Infect Immun* 88.

559 37. Abedon ST, Yin J. 2009. Bacteriophage plaques: theory and analysis. *Methods Mol Biol  
560* 501:161-74.

561 38. Raya RR, H'bert EM. 2009. Isolation of Phage via Induction of Lysogens. *Methods Mol  
562 Biol* 501:23-32.

563 39. Lopes A, Pereira C, Almeida A. 2018. Sequential Combined Effect of Phages and  
564 Antibiotics on the Inactivation of *Escherichia coli*. *Microorganisms* 6.

565 40. Seemann T. 2014. Prokka: rapid prokaryotic genome annotation. *Bioinformatics*  
566 30:2068-9.

567

568